DRAFT VERSION JULY 16, 2018
Preprint typeset using LaTeX style emulateapj v. 01/23/15

EFFECT OF ACTIVE GALACTIC NUCLEI THERMAL HEATING WITH RADIAL DEPENDENCE ON THERMAL STABILITY OF SIMULATED GALAXY CLUSTERS

FORREST W. GLINES [1,2,3], BRIAN W. O'SHEA [1,2], G. MARK VOIT[1]
[1]Department of Physics and Astronomy, Michigan State University, East Lansing, MI 48824, USA
[2]Department of Computational Mathematics, Science and Engineering, Michigan State University, East Lansing, MI 48824, USA and
[3]glinesfo@msu.edu
Draft version July 16, 2018

ABSTRACT

FG: Place holder abstract: Observations from the last decade have revealed the existence of cool-core clusters, galaxy clusters with a cooling time much shorter than the dynamical time. Recent work suggests that clusters may be thermally stable due a central heating mechanism such as an active galactic nucleus (AGN) that prevents cooling. Previous analytical work in one dimension has shown that thermal heating from a central AGN with a power-law radial profile, where the heating exceeds cooling at near and far radii but not in an intermediate region, may produce a stable cluster with an isentropic entropy profile in the core and an isothermal profile outside the cluster. To test this, we simulated idealized galaxy clusters using the ENZO code with thermal heating from a central AGN. Thermal heating as a function of radius was injected proportional to the radius to a fixed exponent in (-3,-2] for each run. Total thermal feedback was set equal to the total rate of cooling in the cluster. Thermal feedback with a conic angular dependence was also explored. However, the purely thermal feedback was not enough to achieve thermal stability and each simulation collapsed due to overcooling. These simulation results support previous work showing that kinetic feedback through a jet in addition to thermal feedback is necessary for self-regulating AGN activity.

1. INTRODUCTION

Active galactic nuclei (AGN,) the super massive black holes at the center of galaxy clusters, are the current most accepted theory for the explanation of cool-core (CC) clusters, galaxy clusters with a peaked X-ray surface brightness. The surface brightness of CC clusters indicate that they are radiating away large amounts of energy away quckly enough that they should have cooling times on the order of 10's of millions of years. This rapid cooling should lead to the condensation of cold clumps of gas within the clusters leading to star formation rates much greater than what is observed. They should collapse quickly within a couple million years, however CC clusters have lifetimes greater than billions of years and constitute roughly half the observed galaxy clusters in the universe. This set of problems is refered to collectively as the "cooling catastrophe." Since CC cluster are common and appear to be stable for at least billions of years, some mechanism must be counteracting the cooling by heating up the core of the cluster and quencing star formation.

Many sources of heating have been explored, including galaxy cluster mergers, cosmic rays, supernovae, and AGN. With the exception of AGN, these sources either do not provide enough heat to offset the cooling or do not heat the cluster on a frequent enough time scale. Observations indicate that the source of heating closely balances the cooling even on short time scales, suggesting a tight coupling between the heating and cooling. Work beginning with (Gaspari et al. 2011b) and later by (Li et al. 2015) and (Meece et al. 2017) demonstrated self-regulating AGN in hydrodynamic simulations of idealized galaxy clusters. All of the simultions used either or both cold-gas and bondi accretion triggered feedback through thermal deposition around the AGN and bipolar outflows from the AGN. Many parameters of this model have been explored, although there is unified agreement for the need of kinetic outflows from AGN Meece Jr (2016); Meece et al. (2017). These AGN regulated the cooling and formation of cold gas within the cluster as well as reproducing temperature, density, and entropy profiles that match observations, including the isentropic multiphase core observed in the $R \approx 100$ kpc of galaxy clusters Gaspari et al. (2012).

The current working model of AGN feedback was built on this simulation work and previous observations Voit et al. (2017); Gaspari et al. (2017); Gaspari & Sądowski (2017). The AGN sits in the middle of a $R \approx 100$ kpc isentropic, thermally and convectively unstable core of multiphase gas at the center of the galaxy cluster. Cold clumps of gas condense out of multiphase region and precipate onto the black hole. The accretion of cold gas onto the AGN triggers feedback through thermal heating around the AGN and kinetic outflows on a larger scale away from the AGN. This feedback maintains the isentropic core and ejects cold clumps of gas into the power-law region of the entropy profile where condensation and overcooling is suppressed. Through cold gas accretion the AGN heating is tightly coupled to the cooling rate while the kinetic outflows disrupt overcooling in the cluster.

However, this model is based on hydrodynamic simulations using simplified AGN feedback while in reality AGN feedback and particularly how the energy thermalizes occurs through a number of effects. These range from turbulent heat diffusion Ruszkowski & Oh (2011), viscous dissipation of waves generated by the AGN Ruszkowski et al. (2004), weak shocks and viscously dissipating sound waves Fabian et al. (2003); **?**, cosmic rays through a number of processes Guo & Oh (2008); Ruszkowski et al. (2017), dissipation of expanding bouyant bubbles created by the AGN Churazov et al. (2001), and many more processes involving turbulence and magnetized plasmas. Although these mechanisms may be necessary to fully model realistic self-regulating AGN in cool-core clusters,

Rather than explore the details of the AGN feedback, this work attempts to further simplify the AGN feedback in order to probe the theoretical model. We abstract the AGN feedback as just thermal heating set equal to the total cooling within the galaxy cluster. We explore a power-law radial dependence to deposit the right amount of energy in each part of the cluster to acheive thermal stability with the initial entropy profile.

Following (Voit et al. 2017), the heating needs to exceed the cooling within the inner core and at large radui, but for the cooling to exceed the heating at intermediate radui where the entropy profile switches from isentropic to a power-low. The multiphase gas should form in the isentropic region, in which cold clumps of gas will condense. The heating in the center pushes these clumps out of the core.

Galaxy clusters have predictable entropy profiles whose shape (although not necessarily normalization) are mass-independent. Cavagnolo et al. (2009) Although -ray observations of the intracluster medium (ICM) indicate that the central cooling times in some galaxy clusters are much shorter than the age of the universe, no cooling catastrophe is observed. This argues that there is a heating mechanism that offsets the cooling and acts on timescales comparable to the cooling time. Given a variety of physical considerations, the primary heating source is largely accepted to be active galactic nuclei (AGN). What is not well-understood, however, is the manner in which AGN deposit energy into the ICM. **The goal of this work** is to constrain the radial dependence of the AGN energy injection by comparing a simplified model of AGN heating with key X-ray observable quantities.

2. METHODOLOGY

2.1. *Simulation Setup*

We ran several simulations of idealized galaxy clusters with a simplified AGN heating model using the cosmology code `Enzo` Bryan et al. (2014). We used the ZEUS solver for hydrodynamics Stone & Norman (1992), due to it's robustness to evolve through discontinuities in the fluid around the AGN with sharply peaked thermal injection. Tablulated cooling was used to model radiative cooling following (Schure et al. 2009), assuming a metallicity of half the solar metallicity. The cooling table has a temperature of 10^4 K, however any processes below this temperature will take place on smaller scale than our spatial resolution. We used a fixed NFW profile for the gravitations potential and ignored self-gravity. Cosmological expansion was also ignored.

The simulations were run on a 3.2 Mpc cube with 64^3 cells in the base grid of the AMR heirachry with a maximum of 8 levels of refinement, making the minimum cell size approximately 195 pc. The mesh was refined at high gradients in the fluid and high baryon density. Additionally, a 4 kpc cube grid centered on the AGN was fixed at the maximum level of refinement.

Each simulation was initialized with temperature and density profiles similar to the Perseus Cluster following (Li & Bryan 2012) and (Meece et al. 2017), which use analytical fits for the temperature profile from (Churazov et al. 2004) and (Vikhlinin et al. 2006) and slightly modified electron number densities following (Mathews et al. 2006). The initial pressure was computed from the temperature and density assuming an ideal gas with $\gamma = 5/3$. The mass giving the fixed gravitational potential has two components: an NFW halo profile and a BCG with a mass profile both following (Li & Bryan 2012), which includes both dark matter and baryonic matter and mimics observations of the Perseus Cluster. The entropy profile of the gas is initialized to

$$K(r) = K_0 + K_{100}\left(r/100\text{ kpc}\right)^{\alpha_K} \tag{1}$$

following results from the ACCEPT database (Cavagnolo et al. 2009), using the definition for specific entropy

$$K \equiv \frac{kT}{n_e^{2/3}}. \tag{2}$$

Each simulation was set to run for 8 Gyr, approximately 4 sound crossing times across the cluster. However, almost all simulations were stopped hydrodynamics solver failed due to high feedback rates introducing discontinuities. A few simulations managed to evolve through the collapse and rebound but with observationally unreasonable final states.

Simulation results were analyzed using `yt` Turk et al. (2011).

2.2. *AGN Feedback*

In the simplified AGN feedback model used here, energy from the AGN is deposited as purely thermal energy in a sphere encompassing the cluster, with the total heating set equal to the total cooling in the cluster. The thermal feedback follows a power law with radius, so that in general, $\dot{e}(r) \propto r^{-\alpha}$. However, this led to several numerical issues, including a feedback that asymtopes to infinity at the AGN and a sharp cutoff in energy at the boundaries of the simulation. These were overcome by adding a minimum radius smoothing length $r_{\rm min} = 1$ kpc (comprising 5 cells in radius on the highest refinement) and an exponential decay at a cutoff radius $r_c = 1$ Mpc. The full form of the volumetric feedback in erg s^{-1} cm^{-3} is

$$\dot{e}(r) = \frac{\dot{E}(t)}{A}\begin{cases}\left(r_{\rm min}/r_c\right)^{-\alpha}\exp\left(-r_{\rm min}/r_c\right) & , \quad r <= r_{\rm min} \\ \left(r/r_c\right)^{-\alpha}\exp\left(-r/r_c\right) & , \quad r > r_{\rm min}\end{cases}, \tag{3}$$

where $\dot{E}(t)$ is the total energy feedback from the energy at time t and A is a scalar to normalize the feedback which is just the integral of the feedback function over the entire feedback radius. Higher values of α correspond to more centralized feedback around the AGN. Without the inner smoothing length, and $\alpha >= 3$ is unnormalizable, corresponding to infinite energy feedback at the origin.

The total AGN heating rate $\dot{E}(t)$ is set to the total cooling rate within the cluster. For simplicity, the heating rate is updated every 10 Myr using `yt` to compute the total cooling. Although the cooling rate increases exponentially up through the cooling collapse, the increase is slow enough so that the heating rate does not fall behind the true cooling rate by more than 1%.

We also investigated a conic feedback when the spherically symmetric feedback models failed to maintain thermally stable galaxy clusters. Outside of the smoothing length $r > r_{\rm min}$, the conic feedback had an additional term to the spherical feedback

$$\dot{e}(\theta) \propto \cos^2\theta \tag{4}$$

where θ is the polar angle. Within $r <= r_{\rm min}$, the conic dependence was removed in order to avoid discontinuities across the origin. The normalization factor A was changed to correctly scale the total heating.

Simulations were run with a range of radial heating distributions ranging from $\alpha = 2.0$ to 2.9. Initially the space of α was probed in increments of 0.1 before more values of α were explored between these values. The later values of α explored differ between the spherically symmetric and conic runs. The values of α explored are listed in table 1.

Figure 1.

Feedback Model	α's explored
Spherical	2.0, 2.1, 2.3, 2.35, 2.375, 2.4, 2.425, 2.45, 2.5, 2.525, 2.55, 2.575, 2.6, 2.8, 2.9
Conic	2.0, 2.1, 2.2, 2.3, 2.325, 2.35, 2.375, 2.4, 2.5, 2.6, 2.7, 2.8

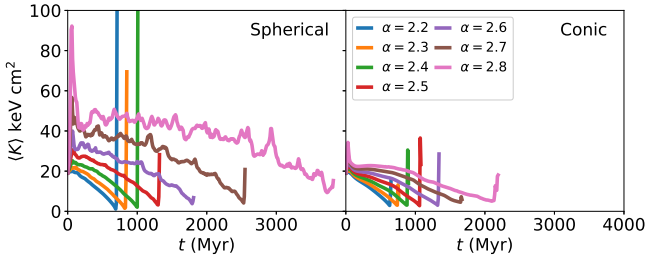

Figure 2. Mean entropy of the inner 10 kpc proper as a function of time for simulations with radial exponents ranging from $\alpha = 2.2$ to $\alpha = 2.8$ with spherical and conic feedback. Mean entropy is calculated by the mass-weighted temperature and the volume-weighted density. To improve visibility, these are plotted up until 30 Myr after the mean core entropy has increased by 60% in a 10 Myr span, or until the simulation has stopped. After this point, the entropy profile has diverged from what would be expected from observations. Simulations using values of α between those shown here were also run, although all exhibited the same core entropy decay with higher values of α decaying slower and conic feedback collapsing faster.

The AGN feedback algorithm used in this work relied heavily and upon and were modified from (Meece Jr 2016; Meece et al. 2017), using the active particle framework built in ();

3. RESULTS

The purely thermal feedback failed to self regulate nor preserve thermal stability. For all choices of α with either spherical or conic feedback, the mean entropy of the inner 10 kpc core fell over time, eventually leading to a cooling driven collapse (fig. 2.) Each simulation formed a cold clump of gas around the core of the cluster (fig. **??**) which began run away cooling and a spike in AGN activity to match the cooling (fig. **??**). Most simulations halted due to hydrodynamics errors during this spike in feedback but a random selection of simulations managed to evolve through the collapse. However, these simulations had raised entropy profiles post-collapse which do not match observed entropy profiles of CC clusters.

3.1. *Formation of Cold Gas*

In all cases with purely thermal heating, a cold clump of gas eventually formed near the center of the cluster. Fig **??** includes entropy and cooling rate versus radius phase plots of the clusters at t = 50 Myr (an arbitrary time step,) when the cold phase gas first appears in the simulation, and at the final step when the either the simulation has reached t = 800 Myr or the hydrodynamics solver has failed. The formation of the cold clump begins with a spreading of the entropy distribution at the radius where the median entropy is minimized. Although the initial entropy profile has an inentropic core, as do observations, the centralized thermal feedback causes the core entropy to peak, leading to a minimal entropy region outside the core. Due to higher energy deposistion and therefore entropy peaks in the centers of high α simulations, the cold gas first forms further from the core for higher α.

When the coldest gas in the distribution reaches a critical specific entropy of around 10^{-1} keV cm^2, the cooling rate accelerates. This gas quickly condenses into the cold phase. As the entropy distribution of the hot phase continues to dip, more gas condenses onto the cold clump in a run away collapse.

Although the heating rate from the AGN ramps up with the accelerated cooling rate, it is unable to immediately warm up nor push out the cold gas. The AGN feedback spikes with the growth of the clump, eventually causing the hydrodynamics solver to crash in most cases.

3.2. *High vs. Low α*

Some differences between simulations arose between simulations using low $\alpha < 2.5$ (more dispered thermal deposition) and high $\alpha > 2.5$ (more centralized thermal deposition.) The high α feedback raised core entropies higher above the initial entropy compared to low α runs by raising core temperatures and pushing out gas to lower electron densities (fig. **??**), as expected. The increased entropy in the core from increased energy deposition delayed the cooling driven collapse for a longer period of time. This was also an expected result. Looking at fig. 2, higher α delayed the collapse super-linearly compared to lower α. However, it should be noted that percent of the total feedback energy deposited in the core does not scale linearly with α but asymptotes exponentially as $\alpha \to 3$. Towards the limiting case as $\alpha \to 3$ the majority of the feedback will constrained to a small $r < 5$ kpc core, similar to the thermal only feedback case from Meece et al. (2017).

3.3. *Mean Core Entropy*

The mean core entropy in all simulations, both with spherical and conic feedback, slowly fell until the formation of the cold clump in all simulations, as is seen in fig. 2. At the formation of the cold clump as the total cooling in the cluster spiked, the AGN activity also spiked, causing the mean core entropy to also spike to unphysically high entropies.

High values of α, or more centrally peaked feedback, maintained a higher core entropy for a longer period of time. Initially the simulation is somewhat stable, however cooling gas on the outskirts of the core lowers the mean core entropy of the inner 10 kpc (see fig. **??**. The conic feedback was less efficient at maintaining core entropy. In all cases, the conic feedback led to a quicker collapse. No quasi-stability was shown for high values of α with conic feedback.

3.4. *Phase Plots*

Fig. 3 shows phase plots of entropy and the cooling rate versus radius. As expected, at t = 500 Myr the higher $\alpha = 2.8$ run has a higher core entropy than $\alpha = 2.2$ since more energy is deposited in the center. The median entropy profile still follows the initial median but there is more high entropy gas near the core. Both the spherical and conic $\alpha = 2.2$ evolved past their collapse but are left with core entropy profiles too high to match observations. The $\alpha = 2.8$ simulations formed cold gas near their cores as they collapsed before hydrodynamic errors stopped the simulations. The heating rate is also plotted with the median cooling in the cooling rate phase diagram. For certain values of α, heating exceeds cooling in the inner core and outer radii but not in the intermediate range where the entropy profile changes from a flat line to a power

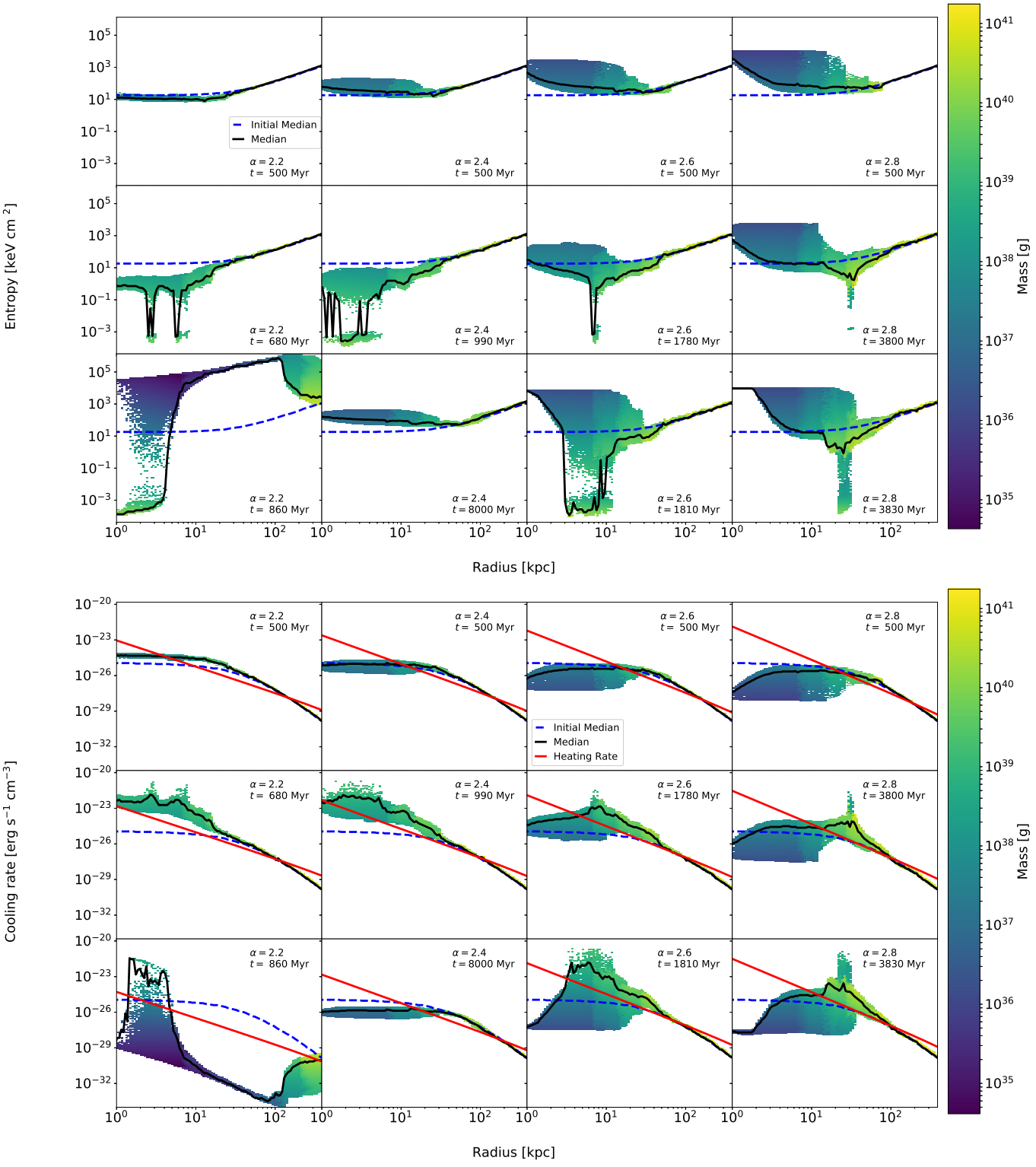

Figure 3. Phase plots of entropy and cooling rate versus radius of simulations with spherical and conic AGN heating with radial exponents $\alpha = 2.2$ and $\alpha = 2.8$ as labeled, with the initial and current median entropy or cooling rate versus radius in dashed blue and solid black respectively. The total heating rate in a shell versus radius is superimposed on the cooling rate in solid red, which is scaled in the simulation to match in total cooling rate. The upper plots are at $t = 500$ Myr and the lower plots are at the final time step of the simulation. ***FG: Should I include the final step? Maybe more a time sequence through collapse of one simulation? Combine r axes. Also, maybe a radial profile of cold gas to see where it forms***

law. ***FG: This would make more sense with volume averaged cooling rate instead of the median - that's what should be directly compared.*** However, this criterion was not enough to produce thermally stable clusters.

4. DISCUSSION

4.1. *Thermal Stability*

In all simulations explored here, the purely thermal heating was unable to prevent a run-away cooling collapse. The distributions of AGN heating did not prevent the formation and growth of cold clumps nor push them out of the core without dumping unphysically high amounts of energy. These shortcomings of a thermal only AGN heating model are in line with simulation work from (Gaspari et al. 2011a; Meece et al. 2017).

High values of α, or more centrally peaked feedback, did prevent the cooling collapse for a longer period.

Comparing to previous work in (Gaspari et al. 2011a; Meece et al. 2017), this current work reaffirms the necessity of kinetic outflows, or at least some mechanism beyond thermal heating, to push cold clumps of gas out of the isentropic zone and into the power-law entropy zone where their condensation may be supressed.

The contrived direct coupling of the AGN feedback to the total cooling rate of the cluster also led to simulation issues when compared to Bondi accretion and cold gas accretion models used in other works Meece et al. (2017). As the gas collapsed into the cool phase, the cooling rate spiked, leading the heating rate to reach unphysically high levels. If the hydrodynamics solver did not fail through the collapse, the high heating rate pushed the isentropic region of the cluster to much higher entropy levels than the initial conditions. Although Bondi accretion and cold gas accretion models increase feedback with the formation of cold gas and higher densities, they do not raise the heating rate to as high levels as seen here.

Higher α, corresponding to more energy input at the cluster core, predictably raised core entropy. Lower α left a flat entropy profiles closer to the initial conditions. The higher α simulations push out enough gas from the core to decrease x-ray brightness.

4.2. *Comparison to Observation*

Although the simulations did not achieve thermal stability, we can still compare some results to observations, particularly entropy and surface brightness profiles from the ACCEPT dataset Cavagnolo et al. (2009).

In fig. 4, we compare the entropy profiles of several representative simulations to entropy profiles from fits from the ACCEPT dataset, as well show surface brightness profiles. Entropy profiles from the simulations were calculated using the mass-weighted temperature and the volume-weighted density, following (). Confidence intervals of entropy profiles from the ACCEPT data were generated using the $K = K_0 + K_{100}\left(r/100\text{ kpc}\right)^{\alpha_k}$ fits. Only CC core clusters are considered, defined here as having $K_0 < 30$ keV cm^2. Simulation data was examined at $t = 500$ Myr, although it should be noted that this is an arbitrary time step. As the higher α simulations drop in core entropy, their entropy profiles will look more similar to the lower α simulations at earlier time steps. The initial conditions chosen also fall outside the ACCEPT dataset, which may affect comparisons.

The simulation data with purely thermal feedback shows

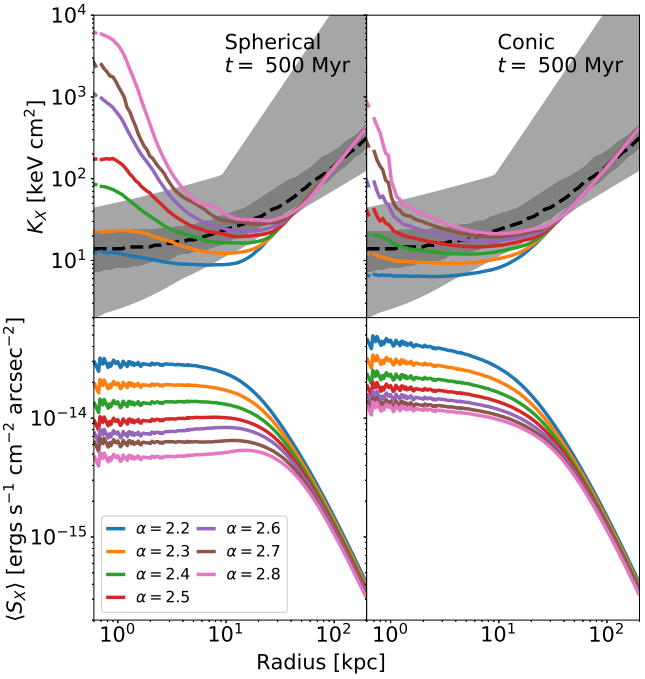

Figure 4. Top: Mean entropy as a function of spherical radius from several representative simulations using different radial exponents α for heating with spherical feedback (left) and conic feedback (right.) Mean entropy is calculated by the mass-weighted temperature and the volume-weighted density. Entropy profiles of CC clusters from the ACCEPT dataset are included in the shaded regions, with the dashed line denoting the median, the darker region denoting the 68% condidence interval, and the lighter region denoting the extent of the CC clusters in the dataset. Entropy profiles from the ACCEPT dataset were generated from the $K = K_0 + K_{100}\left(r/100\text{ kpc}\right)^{\alpha_k}$ fits from the dataset. Only CC clusters defined by $K_0 < 30$ keV cm^2 from ACCEPT are shown, giving 141 clusters. **Bottom:** Mean simulated X-ray surface brightness in the 0.5−2.0keV band of cores of radii $R = 2^0 - 2^4$ proper kpc from as a function of α for heating with spherical feedback (left) and conic feedback (right.) **Bottom:**Mean simulated X-ray surface brightness in the 0.5−2.0 keV band as a function of observing radius from several representative simulations using different radial exponents α for heating with spherical feedback (left) and conic feedback (right.) All data is taken at $t = 500$ Myr.

peaked entropy profiles towards the core, inherently in contrast to the power-law profiles generated from the ACCEPT dataset. The difference is largest for high α, given their centralized feedback. These may be ruled out as an unphysical for simplified models of purely thermal AGN feedback. The lower α simulations may have more acceptable profiles, although even with a small peak in entropy they quickly collapse.

The x-ray surface brightness profiles experience less variation with changes in α. A high α pushes more mass out of the core, leading to less matter to radiate which lowers the surface brightness.

Mean core entropies and surface brightness for different α within different core sizes are shown in fig. 5, with more comparisons to ACCEPT data. The mean core entropy increases with α while the surface brightness decreases. Due to the central entropy peak present in all simulations at $t = 500$ Myr (expect for low α conic simulations, which are beginning to collapse,) the mean core entropy increases with smaller size cores, in contrast to the observed power-laws from ACCEPT where the entropy flattens at the center. Ideally, the mean core entropies should intersect the dashed lines indicated ACCEPT entropy medians at one value α rather than all at wildly different values of α. The central entropy peak prevents this.

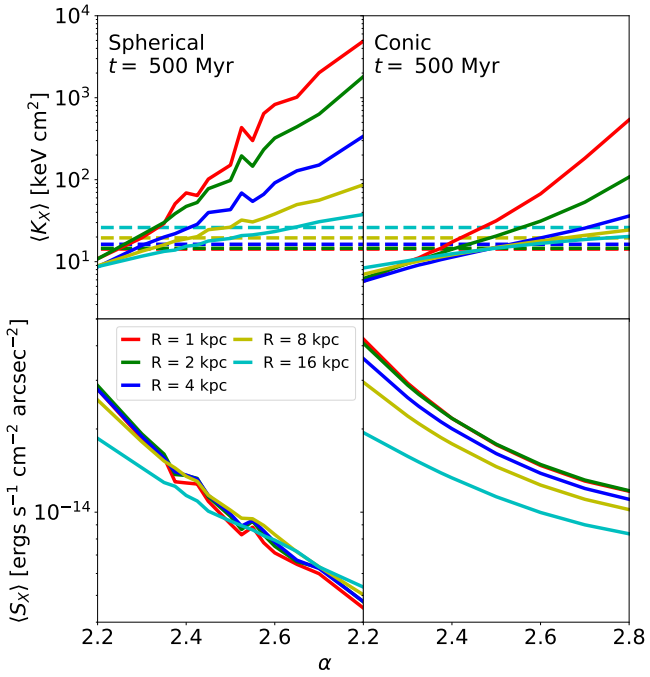

Figure 5. Top: Mean cluster core entropy calculated within impact parameters ranging from $R = 2^0 - 2^4$ proper kpc as a function of α for heating with spherical feedback (left) and conic feedback (right.) Mean entropy from simulation results is calculated by the mass-weighted temperature and the volume-weighted density. Entropy profiles of CC clusters from the ACCEPT dataset are included in the shaded regions, with the dashed lines denoting the mean core entropy within various radii produced from the median entropy profile. Entropy profiles from the ACCEPT dataset were generated from the $K = K_0 + K_{100}\left(r/100\text{ kpc}\right)^{\alpha_k}$ fits from the dataset. Only CC clusters defined by $K_0 < 30$ keV cm^2 from ACCEPT are shown, giving 141 clusters. **Bottom:** Mean simulated X-ray surface brightness in the 0.5−2.0keV band of cores of radii $R = 2^0 - 2^4$ proper kpc from as a function of α for heating with spherical feedback (left) and conic feedback (right.) All data is take at t = 500 Myr.

4.3. *Possible Conclusions*

Due to the failure to produce even quasi-stable clusters with realistic entropy profiles and the absence of a preferred time step in the cluster evolution before the formation of the cold phase, comparisons to observation may not be accurate. However, a few possible conclusions can be made.

In the context of purely thermal AGN feedback, highly centrally concentrated feedback (corresponding to high $\alpha > 2.5$ simulations) produce unphysically high entropy cores. These may be ruled out from simplified AGN feedback models.

When the heating rate was directly tied to the total cooling rate in the cluster, the rapid cooling of gas into cold clumps caused the heating rate to reach unphysically high levels. This is in contrast to simulations using Bondi accretion and cold gas accretion such as in Meece et al. (2017), where the AGN feedback still increases with the formation of cold gas but can be tuned to stay within physically reasonable values.

The basic power-law AGN thermal heating considered here are unable to maintain thermal stability of the cluster. In cases, when a cold clump of gas forms, the simulation is unable to disrupt the clump without injecting unphysically high amounts of energy. The thermal heating in these simulations was unable to replace kinetic outflows from AGN jets such as in (Meece et al. 2017). However, a purely thermal model may still exist, although with more parameters and constraints, which can mimic observed CC clusters.

5. SUMMARY

We have presented simulation results for simplified models of AGN feedback using purely thermal feedback following a radial power law, $\dot{e} \propto r^{-\alpha}$ dependence, where the total feedback is scaled to the total cooling within the clusters. All cases of this setup failed to maintain thermal stability with observationally reasonable entropy profiles (figs. 2 3. The purely thermal feedback was unable to suppress the formation of a large cold clump of gas while the increased cooling rate through this process raised the heating rate to very high levels.

We also compared entropy profiles from these results to observational data from the ACCEPT dataset. Our simulations exhibited small to large central peaks in entropy which differ from the power-law entropy profiles from ACCEPT. The entropy peaks were more pronounced for higher values of α due to the more centralized feedback. Simplified AGN models with centralized thermal heating are unlikely to produce realistic entropy profiles.

A few possible conclusions are as follows:

- Highly centralized feedback produces unreasonable high entropy profiles compared to observations. These can a eliminated from simplified models of AGN feedback.
- An AGN heating rate directly tied cooling rate led to a sharp jump in feedback as cold gas formed in the simulation. This differs from previous simulations approximating feedback rates using Bondi and cold gas accretion models, which can temper the feedback.
- No configuration of purely thermal feedback explored here achieved thermal stability nor prevented a run away collapse into a cold clump, in contrast to previous simulations included kinetic jets.

6. ACKNOWLEDGMENTS

This project has been supported by NASA through Astrophysics Theory Program grant #NNX15AP39G and Hubble Theory Grant HST-AR-13261.01-A, and by the NSF through grant AST-1514700. The simulations were run on the NASA Pleiades supercomputer through allocation SMD-16-7720. `Enzo` and `yt` are developed by a large number of independent researchers from numerous institutions around the world. Their commitment to open science has helped make this work possible.

REFERENCES

Bryan, G. L., et al. 2014, The Astrophysical Journal Supplement Series, 211, 19
Cavagnolo, K. W., Donahue, M., Voit, G. M., & Sun, M. 2009, The Astrophysical Journal Supplement Series, 182, 12
Churazov, E., Brüggen, M., Kaiser, C. R., Böhringer, H., & Forman, W. 2001, The Astrophysical Journal, 554, 261
Churazov, E., Forman, W., Jones, C., Sunyaev, R., & Böhringer, H. 2004, Monthly Notices of the Royal Astronomical Society, 347, 29
Fabian, A. C., Sanders, J. S., Allen, S. W., Crawford, C. S., Iwasawa, K., Johnstone, R. M., Schmidt, R. W., & Taylor, G. B. 2003, Monthly Notices of the Royal Astronomical Society, 344, L43
Gaspari, M., Brighenti, F., D'Ercole, A., & Melioli, C. 2011a, Monthly Notices of the Royal Astronomical Society, 415, 1549
Gaspari, M., Melioli, C., Brighenti, F., & D'Ercole, A. 2011b, Monthly Notices of the Royal Astronomical Society, 411, 349

Gaspari, M., Ruszkowski, M., & Sharma, P. 2012, The Astrophysical Journal, 746, 94
Gaspari, M., & Sądowski, A. 2017, The Astrophysical Journal, 837, 149
Gaspari, M., Temi, P., & Brighenti, F. 2017, Monthly Notices of the Royal Astronomical Society, 466, 677
Guo, F., & Oh, S. P. 2008, Monthly Notices of the Royal Astronomical Society, 384, 251
Li, Y., & Bryan, G. L. 2012, The Astrophysical Journal, 747, 26
Li, Y., Bryan, G. L., Ruszkowski, M., Voit, G. M., O'Shea, B. W., & Donahue, M. 2015, The Astrophysical Journal, 811, 73
Mathews, W. G., Faltenbacher, A., & Brighenti, F. 2006, The Astrophysical Journal, 638, 659
Meece, G. R., Voit, G. M., & O'Shea, B. W. 2017, The Astrophysical Journal, 841, 17pp
Meece Jr, G. R. 2016, AGN Feedback and Delivery Methods for Simulations of Cool-Core Galaxy Clusters (Michigan State University)
Ruszkowski, M., Brüggen, M., & Begelman, M. C. 2004, The Astrophysical Journal, 611, 158
Ruszkowski, M., & Oh, S. P. 2011, Monthly Notices of the Royal Astronomical Society, 414, 1493
Ruszkowski, M., Yang, H.-Y. K., & Zweibel, E. 2017, The Astrophysical Journal, 834, 208
Schure, K. M., Kosenko, D., Kaastra, J. S., Keppens, R., & Vink, J. 2009, Astronomy & Astrophysics, 508, 751
Stone, J. M., & Norman, M. L. 1992, The Astrophysical Journal Supplement Series, 80, 753
Turk, M. J., Smith, B. D., Oishi, J. S., Skory, S., Skillman, S. W., Abel, T., & Norman, M. L. 2011, The Astrophysical Journal Supplement Series, 192, 9
Vikhlinin, A., Kravtsov, A., Forman, W., Jones, C., Markevitch, M., Murray, S. S., & Van Speybroeck, L. 2006, The Astrophysical Journal, 640, 691
Voit, G. M., Meece, G., Li, Y., O'Shea, B. W., Bryan, G. L., & Donahue, M. 2017, The Astrophysical Journal, 845, 80